Time-Resolved Study of Nonlocal Electron Heat Transport in High Temperature Plasmas

T. Ditmire,[1,*] E. T. Gumbrell,[1] R. A. Smith,[1] A. Djaoui,[2] and M. H. R. Hutchinson[1,2]
[1]*Imperial College of Science, Technology and Medicine, Blackett Laboratory, London, SW7 2BZ, United Kingdom*
[2]*Rutherford Appleton Laboratory, Chilton, Didcot, Oxfordshire OX11 0QX, United Kingdom*
(Received 11 August 1997)

Exploiting the high absorption efficiency of intense, ultrashort laser pulses in gases of atomic clusters we have created plasma filaments with temperatures of >1 keV and electron densities in excess of 10^{20} cm^{-3}. Using picosecond laser pulses, we have interferometrically measured the temporal and spatial evolution of the electron density in these plasmas on a fast (<50 ps) time scale. Our measurements indicate that nonlocal heat transport by hot electrons drives a fast ionization wave, and the data agree well with a nonlocal heat transport model. [S0031-9007(97)05139-9]

PACS numbers: 52.40.Nk

The mechanisms for heat transport in high temperature laser produced plasmas have been a topic of extensive research. The importance of nonlocal heat transport effects due to hot electrons in these plasmas was identified some years ago and a substantial amount of theoretic work has been conducted to understand its consequence [1–4]. Some experimental confirmation of these effects has been performed using long pulse (>500 ps) irradiation of solid targets [5], although, most experiments have been limited to the observation of indirect consequences such as the effect on the mass ablation rate [6]. Interpretation of these measurements are complicated when long pulse lasers are used since the pulses deposit energy in the plasma on the time scale of the heat transport dynamics. Intense, ultrashort (ps or fs) laser pulses, however, make possible clean, time-resolved studies of heat transport phenomena [7,8] and are ideal for more direct measurement of nonlocal transport effects.

Recent studies on the interaction of intense short pulses with gases of atomic clusters have suggested a unique method to produce high temperature plasmas of interest for these transport studies [9,10]. It has been shown that a gas of modest mean atomic density composed of atomic clusters with of the order of 1000 atoms/cluster exhibits between 50% and 100% absorption of the laser energy within a focal volume [11]. This is made possible by the high local density within the cluster and is in contrast to a gas of monomers in which the absorption of intense laser light is very low. Consequently plasmas with temperatures of >1 keV can be easily created on a fast time scale. When the intense laser pulse is focused through the cluster medium, the heated clusters explode leaving a hot plasma filament with a diameter of the order of the focus spot size ($20-100$ μm) and length of the order of the laser confocal parameter (>1 mm). In this Letter we present a study of the dynamics of heat transport from the keV plasmas produced in these clustering gases. Using short pulse laser interferometry we have temporally and spatially resolved the electron density profiles of the hot plasma filament. We observe a heat transport driven radial ionization wave on a time scale much faster than the hydrodynamic expansion of such plasmas [12], and we find that this energy transport is dominated by nonlocal effects. Through comparison with numerical modeling our measurements provide a direct experimental comparison with the previously published theory of Luciani *et al.* [1,4] on nonlocal electron transport.

In plasmas with modest temperature gradients the energy transport is usually dominated by electron diffusive heat transport. In this regime the heat conductivity is given by the usual Spitzer formula [13]. However, when the heat gradients in the plasma are large the diffusive approximation breaks down. This failure occurs when the mean free path of the electrons approaches the spatial scale of the temperature gradient. In this regime the heat transport is dominated by hot electrons free streaming from the hot portions of the plasma to the cooler regions, and the Spitzer-Härm conductivity formula exceeds the maximum possible free-streaming electron conduction rate (given as $q_{fs} = 3n_e T_e^{3/2}/2m_e^{1/2}$). This regime is usually modeled by clamping the heat conductivity to a value given by fq_{fs}, where f is an empirical constant less than one, called the flux limiter [14]. To more accurately model the effects of this regime of heat transport a semiempirical formula for the nonlocal energy transport was proposed by Luciani *et al.* [1]. Calculations using this formula have been shown to be in good agreement with more detailed Fokker-Planck simulations of electron energy transport in steep gradients and deviate substantially from simple flux-limited transport calculations [2,4].

In the laser heated clustering gases, the temperatures can be in the vicinity of 1 keV, the scale lengths are of the order of $10-50$ μm, and the electron densities are between 10^{19} and 10^{20} cm^{-3}. Thus, using the usual formula for 90° scattering of electrons [14], we find that the electron mean free path is $1-10$ times the plasma gradient indicating that these plasmas are ideal for exploring the dynamics of the nonlocal transport. Furthermore, using a picosecond heating pulse decouples the fast heating of the plasma from the subsequent energy transport.

 0031-9007/98/80(4)/720(4)$15.00

In our experiments the clustering medium was produced with a pulsed gas jet which delivered a gas plume with an average atomic density of up to 1.5×10^{19} cm^{-3}. Under these conditions we can produce argon clusters with average cluster diameter of 80 Å (corresponding to about 5000 Ar atoms/cluster). We can also cryogenically cool the gas jet which allows us to produce clusters of hydrogen or deuterium, gases which do not form clusters at room temperature. The cluster gas was heated with a Nd:glass laser system based on chirped pulse amplification which produced transform-limited 2 ps pulses. These pulses were frequency doubled to 526 nm and focused to a Gaussian spot diameter ($1/e^2$) of 50 μm into the gas jet, yielding a peak intensity in vacuum of $\sim 10^{16}$ W/cm^2.

Under these conditions roughly 60% of the total incident laser energy of 300 mJ was absorbed by the gas within the focal volume (which was $\sim 4 \times 10^{-6}$ cm^{-3}) [11]. For an argon gas with an atomic density of 1.5×10^{19} cm^{-3} and an average ionization state of 8+ (Ne-like), this absorbed energy fraction implies an initial electron temperature of $\sim$1.5 keV assuming equal electron and ion temperatures. This value is consistent with previous measurements of electron and ion energies resulting from the explosion of laser heated clusters [15,16].

To probe the plasma filament, a small amount of the main 2 ps, 526 nm pulse was split off and Raman shifted in ethanol to a wavelength of 620 nm. This pulse traversed a delay leg and illuminated the plasma filament at a right angle to the propagation direction of the main pulse. The plasma was imaged onto a charge-coupled device (CCD) camera (yielding a spatial resolution of 2.5 μm). Between the imaging telescope and the CCD detector the probe light passed through a Michelson interferometer with a roof prism in one leg such that probe light which traversed the plasma filament was interfered with reference light which passed below the plasma. The interferograms yield information on the phase shift resulting from the passage of the light through a chord across the cylindrically symmetric plasma. This phase shift can be Abel-inverted to yield the radial electron density profile.

Figure 1 shows interferometric images of the plasma filament created in an argon cluster gas at four different times with respect to the main heating pulse. $t = 0$ is defined as the point at which the gas is ionized by the peak of the laser pulse. 3 ps before the peak of the pulse a small amount of ionization due to the rising edge of the laser pulse is evident from the small deviation of the fringes along the center axis of the image. At $t = 0$ rapid ionization by the main laser pulse in the center of the image on a time scale comparable to the probe pulse width causes the fringes to smear out. From this image it is clear that the gas is initially ionized to a radius of slightly greater than 50 μm. Because of the low ionization threshold of the argon ($\sim 2 \times 10^{14}$ W/cm^2) the gas is ionized out in the spatial wings of the laser focus, however, assuming a Gaussian focal spot distribution this implies that the bulk

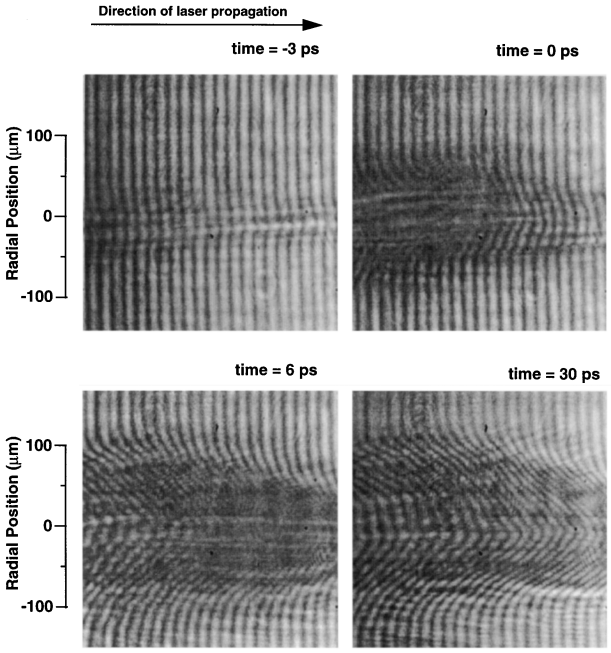

FIG. 1. Interferometric images of the plasma filament created in an argon cluster gas at four different times with respect to the main heating pulse. The heating pulse had an energy of 300 mJ.

of the laser energy is deposited within a cylinder of roughly 20–30 μm in radius. Within 6 ps after heating by the main pulse, energy transport from the central hot plasma has driven ionization out to a radius of over 100 μm.

The deconvolved electron density profiles in the argon plasma at 2 times are shown in Fig. 2. Since the initial radius of the ionization is $\sim$50 μm, these data indicate that the velocity of the ionization wave driven by the hot electrons is of the order of 1×10^7 m/s. This is roughly consistent with the velocity of free-streaming thermal electrons in a 1.5 keV plasma (1.6×10^7 m/s). At the center of the plasma the measured electron density is 1.3×10^{20} cm^{-3}, indicating that the argon is about eight times ionized.

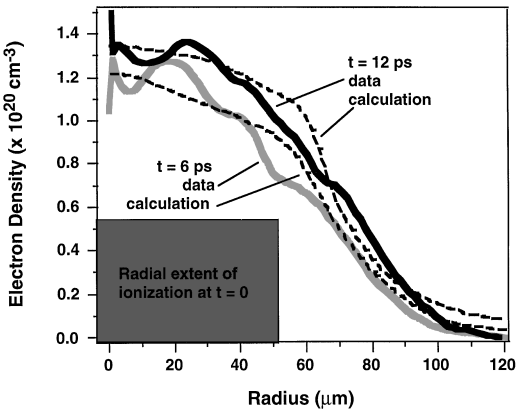

FIG. 2. Deconvolved electron density profiles measured in the argon plasma at two times (solid lines). The dashed lines are the results of the MED103 calculation including the effects of nonlocal electron heat transport.

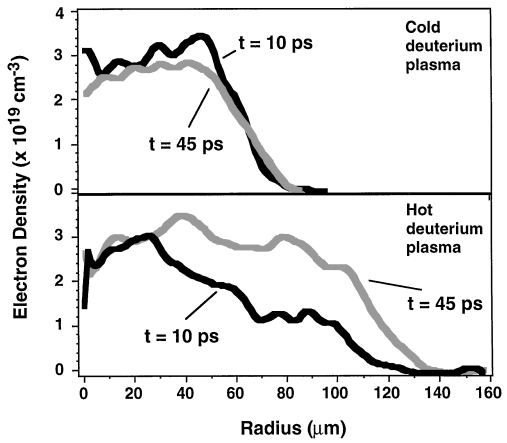

FIG. 3. Measured electron density profiles in deuterium gas at two times. The top image is from a plasma that initially contained no clusters and was therefore cold. The bottom image is of plasma created in a gas containing D_2 clusters in which the laser absorption was high and the initial plasma temperature was high.

To illustrate the importance of the presence of hot electrons on the plasma transport dynamics, the plasma profiles at two times in a deuterium plasma are shown in Fig. 3. In the first case the plasma is created in a gas of only D_2 molecules from the gas jet at room temperature, a case in which the laser absorption is very low ($<3\%$) and the plasma temperature is expected to be of the order of 20–30 eV. In the second case, the evolution of a plasma created in deuterium clusters is illustrated, produced when the gas jet is cooled to $-170\,^{\circ}\mathrm{C}$. Here the laser absorption is large ($>80\%$) and the plasma is hot. The low temperature deuterium plasma exhibits a flattop profile, a result of complete ionization of the gas by the laser at $t = 0$, with no evidence for a fast radial heat wave at a later time. The high temperature plasma, however, exhibits a fast ionization wave traveling outward from the initial plasma in a manner similar to that seen in the argon plasma.

To derive information on the spatial extent of the hot plasma we have also conducted time integrated pinhole camera measurements of x rays emitted from the argon plasmas. We used a camera with a 20 μm pinhole and a magnification of 12. The pinhole is covered with a filter consisting of 0.8 μm of Formvar and 0.5 μm of Al which blocks photons with energy below about 0.5 keV. Figure 4 shows the image of the Ar emission under the same conditions as Figs. 1 and 2. This image indicates that the plasma emits x rays with energy above 0.5 keV out to a radius of 100 μm, much larger than the initial 30–50 μm radius of the energy deposition, confirming that substantial radial heat transport occurs.

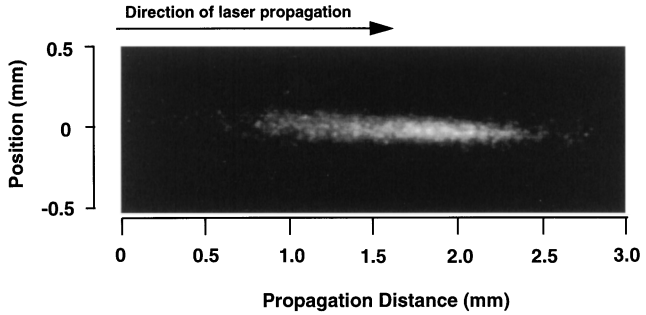

FIG. 4. Pinhole camera image of x rays with energy above 0.5 keV from the argon plasma.

To explore the effects of heat transport in our experiments and to test the importance of nonlocal effects we have modeled our data using the Lagrangian plasma code MED103 [17]. A cylindrical geometry is assumed and an ideal gas equation of state is used for the electrons and the ions. This code includes all of the equations for hydrodynamic motion of the plasma (though we emphasize that virtually no hydrodynamic motion occurs on the time scales considered here) and the heat transport due to the standard Spitzer-Härm formulation.

Because the temperatures are high and the densities are modest, the ionization state of the plasma will not be in local thermodynamic equilibrium on the time scales considered. Consequently the plasma ionization and excitation in our model are governed by time dependent population rate equations with an average atom model. To examine the accuracy of the Luciani, Mora, and Virmont model of the nonlocal heat transport we have included their formulation in our calculations. We use a variation of their original formula to account for transport in cylindrical coordinates [18]. The total radial heat flow is given by

$$q_{\mathrm{nonlocal}}(r) = \frac{1}{\beta}\int_{-R}^{R} q_{\mathrm{Spitzer}}(r')G(r,r')\,dr', \qquad (1)$$

$$G(r,r') = \frac{1}{64\lambda_e(r')}\exp\left[-\frac{1}{32n_e(r')\lambda_e(r')}\int_{r'}^{r} n_e(r'')\,dr''\right]\min(1, r'/r)\,dr', \qquad (2)$$

where $q_{\mathrm{Spitzer}}(r)$ is the standard Spitzer heat flow [13] and $\beta = \int_{-R}^{R} G(r,r')\,dr'$. ($R$ is the radial extent of the plasma.) Here the standard electron-ion scattering mean free path is used in regions of the plasma when the ionization state of the plasma is >1 and modified to account for the impact ionization cross section in unionized regions of the gas.

To model our data we assume that the energy is deposited instantaneously by the laser, and we start with an argon plasma that has Gaussian temperature and electron density profiles with 35 μm, $1/e^2$ radii. The electron and ion temperatures are initially set to be equal, though we find that the dynamics are virtually identical if we assume that the ions are cold. We chose a peak temperature on axis of 1.5 keV, an atomic density of 1.5×10^{19} cm^{-3}, and the initial charge state of the argon on axis as 8+. These initial conditions are consistent with the measured total energy deposition by the laser, the initial observed

ionization radius, and the measured initial charge state of the argon at early times.

An example of a calculation with these initial conditions is shown in Fig. 5. This shows the electron density radial profiles at three different times calculated accounting for the effects of nonlocal transport. For comparison, the calculated plasma evolution for the same initial conditions when the effects of nonlocal heat transport are not included is also shown in this illustration. For this calculation we utilize flux-limited transport with a maximum physical flux limiter of 1.0. From the evolution of the plasma in the presence of nonlocal transport the evolution is composed of two stages. Within 6 ps of the initial energy deposition, the temperature gradient is very large. The nonlocal transport term is responsible for fast heating of the cold gas surrounding the hot core on a 2–6 ps time scale. The heat transport is accompanied by a rapid fall in temperature in the center of the plasma to 500 eV. This transport drives a radial ionization wave with a velocity of around $\sqrt{k_B T_e/m_e} \approx 10^7$ m/s.

The fast ionization wave seen in the nonlocal calculation is not present in the flux-limited Spitzer case. Only the slower increase in electron density is evident. Furthermore, we see that the extent of ionization in the radial direction does not increase, nor does it yield the electron density tail at large radii seen in the nonlocal calculation. The presence of this ionization tail in the cold material adjacent to a hot plasma is the result of free-streaming hot electrons and was predicted in the original modeling of nonlocal effects in Ref. [1].

A comparison of these calculations with the time resolved electron density data confirm the importance of nonlocal heat transport effects. First we see in Fig. 1 that the observed extent of ionization expands by 50 μm in under 6 ps. This is very similar to the ionization wave driven by nonlocal transport seen in the calculation of Fig. 5. It is also apparent that the tail in the radial profile of the measured electron density 6 ps after heating the plasma is very similar to that tail predicted by the nonlocal transport model. Plotted in Fig. 2 are the calculated electron density profiles for comparison with the experimental profiles. We see that the nonlocal heat transport model quite accurately predicts the shape and extent of this tail. Finally we point out that the predicted extent of the plasma after the nonlocal heat conduction within the initial 10 ps is very similar to the radial extent of the x-ray emission from the argon plasma measured with the pinhole camera (Fig. 3), increasing from 50–100 μm.

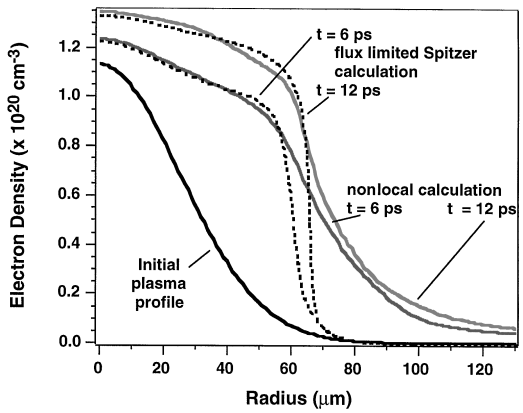

FIG. 5. Calculated electron density profiles resulting from an Ar plasma with the initial density profile shown and an initial peak electron and ion temperature of 1.5 keV. The solid lines show the evolution of the plasma profile when nonlocal transport effects are included in the calculation and the dashed lines show the calculated profile when flux-limited diffusive transport is used.

In conclusion, we have presented time- and space-resolved images of moderate density plasma filaments with initial temperature of >1 keV. Comparison of these measurements with modeling including nonlocal electron heat transport indicates that the more conventional treatment of flux-limited diffusive heat transport is inadequate in predicting the heat flux or the spatial extent of the plasma x-ray emission. These results emphasize the importance of using a nonlocal formulation of heat transport when plasma temperature gradients are large.

We acknowledge the assistance of N. Ditmire, useful conversations with J. W. G. Tisch, and the technical support of P. Ruthven and A. Gregory.

*Current address: Lawrence Livermore National Laboratory, L-440, Livermore, CA 94550.

[1] J. F. Luciani, P. Mora, and J. Virmont, Phys. Rev. Lett. **51**, 1664 (1983).
[2] P. A. Holstein, J. Delettrez, S. Skupsky, and J. P. Matte, J. Appl. Phys. **60**, 2296 (1986).
[3] A. Bendib, J. F. Luciani, and J. P. Matte, Phys. Fluids **31**, 711 (1988).
[4] P. Mora and J. F. Luciani, Laser Part. Beams **12**, 387 (1994).
[5] P. Alaterre *et al.*, Phys. Rev. A **32**, 324 (1985).
[6] T. J. Goldsack *et al.*, Phys. Fluids **25**, 1634 (1982).
[7] B. T. Vu, A. Szöke, and O. L. Landen, Phys. Rev. Lett. **72**, 3823 (1994).
[8] T. Ditmire, E. T. Gumbrell, R. A. Smith, L. Mountford, and M. H. R. Hutchinson, Phys. Rev. Lett. **77**, 498 (1996).
[9] A. McPherson *et al.*, Nature (London) **370**, 631 (1994).
[10] T. Ditmire, T. Donnelly, R. W. Falcone, and M. D. Perry, Phys. Rev. Lett. **75**, 3122 (1995).
[11] T. Ditmire, R. A. Smith, J. W. G. Tisch, and M. H. R. Hutchinson, Phys. Rev. Lett. **78**, 3121 (1997).
[12] M. Dunne *et al.*, Phys. Rev. Lett. **72**, 1024 (1994).
[13] L. Spitzer and R. Härm, Phys. Rev. **89**, 977 (1953).
[14] W. L. Kruer, *The Physics of Laser Plasma Interactions* (Addison-Wesley, Redwood City, 1988).
[15] Y. L. Shao *et al.*, Phys. Rev. Lett. **77**, 3343 (1996).
[16] T. Ditmire *et al.*, Nature (London) **386**, 54 (1997).
[17] A. Djaoui, Rutherford Appleton Laboratory Internal Report No. RAL-TR-96-099, 1996.
[18] A. Djaoui and A. A. Offenberger, Phys. Rev. E **50**, 4961 (1994).